Energy-resolved pulse profile changes in V 0332+53: indications for cyclotron wings emission

Antonino D'Aì, Dimitrios K. Maniadakis, Carlo Ferrigno, Elena Ambrosi, Ekaterina Sokolova-Lapa, Giancarlo Cusumano, Peter A. Becker, Luciano Burderi, Melania Del Santo, Tiziana Di Salvo, Felix Fürst, Rosario Iaria, Peter Kretschmar, Valentina La Parola, Christian Malacaria, Ciro Pinto, Fabio Pintore, and Guillermo A. Rodriguez-Castillo.

Abstract: We investigate changes in the pulse profile at the cyclotron line energy of the accreting X-ray pulsar V0332+53 by analyzing the energy-resolved pulse profile behavior in NuSTAR observations and studying the energy dependence of the pulse profiles. The pulsed fraction spectra, constructed as described in Ferrigno et al. (2023), reveal two Gaussian-shaped features on either side of the cyclotron line energy in the energy spectrum. These two features do not show significant variation with source luminosity. We interpret them as evidence of cyclotron emission wings (or shoulders), which are predicted by theoretical models of line formation for resonant cyclotron absorption. To explain these results, we propose a possible system geometry for V0332+53: the line of sight is nearly aligned with the spin axis, while the magnetic axis is either aligned with or, more likely, orthogonal to the spin axis.

V0332+53 is a recurrent outbursting young X-ray pulsar (Terrell & Priedhorsky 1984). It forms a Be/X-ray binary system with the O8-9Ve star BQ Cam (Honeycutt & Schlegel 1985; Negueruela et al. 1999), and has exhibited several giant X-ray outbursts since its discovery. During the 1989 outburst, a cyclotron resonant scattering feature (CRSF) at ∼28.5 keV (corresponding to a magnetic field strength of 3×10^{12} G) was discovered (Makishima et al. 1990). In the giant outburst that began in November 2004, monitored by RXTE and INTEGRAL (Mowlavi et al. 2006; Tsygankov et al. 2006, 2010), three CRSFs were detected at ∼27 keV, ∼51 keV, and ∼74 keV (Pottschmidt et al. 2005). The most recent giant outburst in 2015 was observed with the Burst Alert Telescope on board the Swift Neil Gehrels Observatory (Cusumano et al. 2016), as well as with NuSTAR (Doroshenko et al. 2017; Vybornov et al. 2018) and INTEGRAL (Ferrigno et al. 2016).

We applied the methods described in Ferrigno et al. (2023) to investigate the energy dependence of the pulse profiles, constructing the pulsed fraction spectra (PFS) for V0332+53 using NuSTAR data from the 2015 outburst. Figure 1 shows the light curve of this outburst, recorded by the Swift/BAT in the 15–50 keV range, with NuSTAR observations (red points) marked for the duration of the outburst. This analysis is limited to the first four NuSTAR observations (ObsId 802, 804, 806, and 808), as the last three observations have insufficient statistics to produce a reliable PFS.

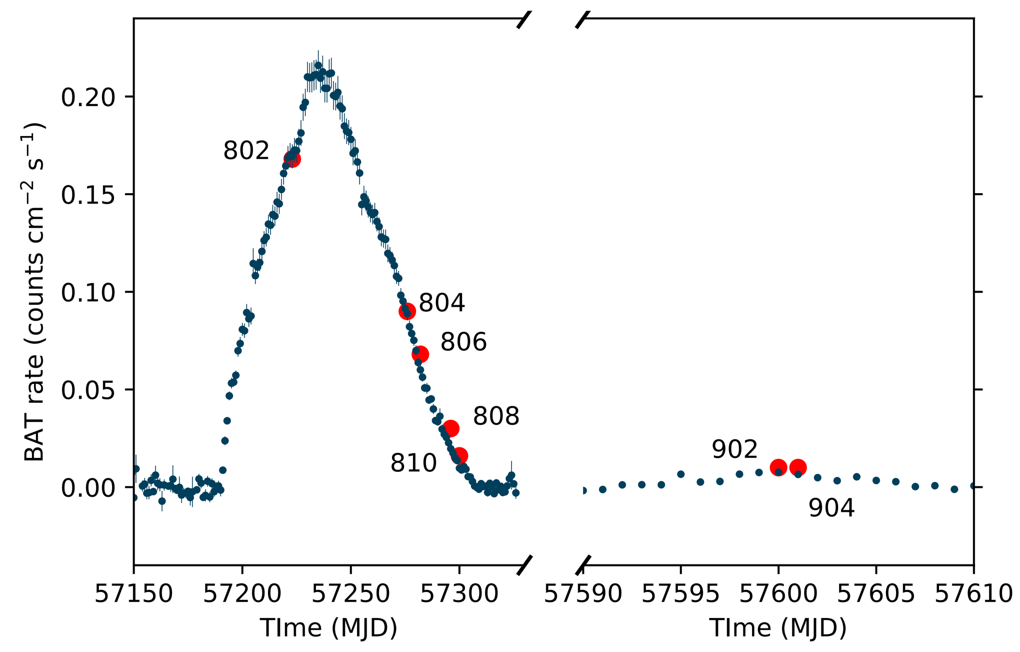

Fig. 1. Swift/BAT light curve of V 0332+53 during its 2015 outburst with superimposed the NuSTAR observations performed on 2015 and two observation on 2016. All NuSTAR observation are marked by the red points.

Figure 2 shows the resulting PFS for the selected observations. We model the pulsed fraction (PF) continuum using a polynomial function. To avoid using a high-order polynomial that might overfit the data and better capture the shapes of local features, we split the fit into two energy bands: a low-energy and a high-energy band. The energy range for the split E_{split} is chosen to be between 10–15 keV (see Ferrigno et al. 2023 for more details). The polynomial order is selected such that the fitted model yields a p-value greater than 0.05. In the high-energy portion of the PFS, where local features are clearly visible, we model these features using Gaussian profiles. The line centroid, width, and amplitude are treated as free fitting parameters.

All PFS share some common characteristics, which appear to be only weakly dependent on the accretion state. The PF values below E_{split} are generally very low (< 0.1), especially when compared to other well-known accreting binaries (e.g., Ferrigno et al. 2023). These values tend to show a global minimum around 8–12 keV. After this minimum, the PF begins to increase following a linear trend, which is then interrupted by the presence of a complex structure that we model as two Gaussians with positive amplitudes. The best-fitting parameters and their associated errors for the PFS are reported in Table 1.

The two peaks exhibit variations in their relative amplitudes, while their separation, relative to the spectral position of the fundamental cyclotron line (Doroshenko et al. 2017), remains constant. For reference, we will refer to these PFS features as the red and blue peaks, based on their position relative to the cyclotron line. After the blue peak, the PF values increase again in the two brightest observations (802 and 804), while for the remaining observations, the lack of sufficient statistics prevents us from identifying a clear pattern.

The energy positions of the peaks consistently lie on either side of the cyclotron line in all NuSTAR observations and follow the same trend as the fundamental cyclotron line energy with luminosity (Cusumano et al. 2016). However, the ratio of the peak amplitudes varies: as the source luminosity decreases, the red peak amplitude increases, while the blue peak amplitude shows little to no significant variation.

	ObsID 802	ObsID 804	ObsID 806	ObsID 808
$X^2_{red,low}$/d.o.f.	1.4/48	1.2/42	1.0/43	1.5/36
$X^2_{red,high}$/d.o.f.	0.8/28	1.7/36	1.2/36	1.6/17
$n(high)_{pol}$	1	3	3	1
$n(low)_{pol}$	5	3	1	2
E_{split}(keV)	14.97	11.33	10.01	11.81
A1	0.049 +/- 0.014	0.36 +/- 0.04	0.38 +/- 0.02	1.02 +/- 0.05
E1(keV)	25.1 +/- 0.3	25.74 +/- 0.3	25.78 +/- 0.3	26.62 +/- 0.3
σ_1(keV)	0.94 +/- 0.18	1.48 +/- 0.14	1.20 +/- 0.06	1.79 +/- 0.09
A_2	0.52 +/- 0.04	0.70 +/- 0.05	0.66 +/- 0.05	0.45 +/- 0.08
E_2(keV)	30.49 +/- 0.11	30.44 +/- 0.10	30.28 +/- 0.11	31.70 +/- 0.24
σ_2(keV)	1.63 +/- 0.11	1.63 +/- 0.12	1.68 +/- 0.14	0.98 +/- 0.17
D_{cyc}	0.863 +/- 0.002	0.861 +/- 0.002	0.862 +/- 0.002	0.899 +/- 0.003
E_{cyc} (keV)	27.93 +/- 0.02	28.25 +/- 0.02	28.40 +/- 0.02	29.03 +/- 0.04
σ_{cyc} (keV)	8.47 +/- 0.08	7.59 +/- 0.08	7.59 +/- 0.08	6.73 +/- 0.08

Table 1. PFS best-fit parameters of the V0332+53 for observations 802, 804, 806, and 808. The CRSF parameters at the bottom of each column are taken as reference from Doroshenko et al. (2017).

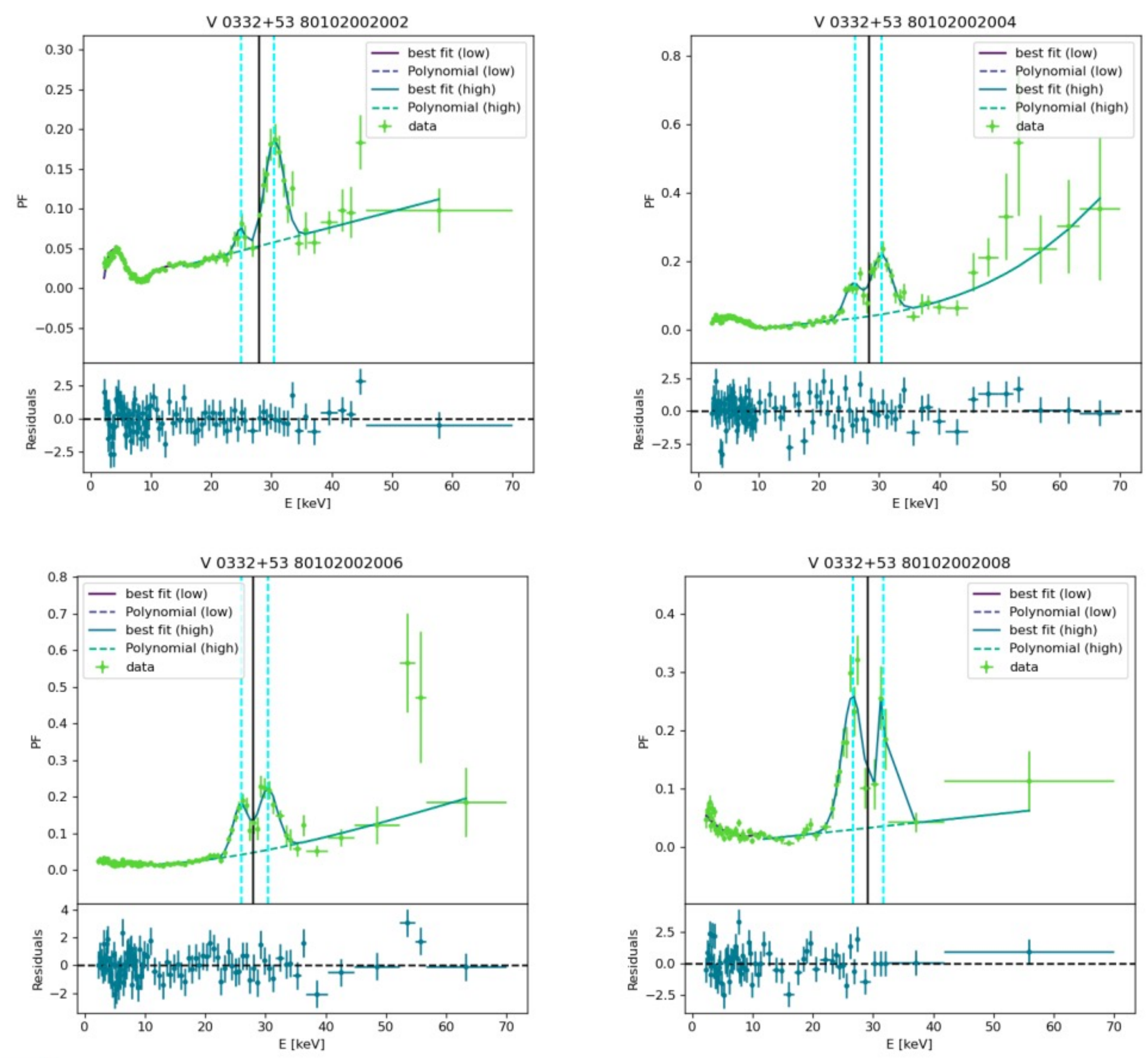

Fig. 2. PFS, best-fitting models and residuals for ObsID 802, 804, 806 and 808. Cyan dashed lines mark energy positions of the Gaussian peaks. The black line marks the energy of the fundamental cyclotron line (from Doroshenko et al. 2017).

Two main characteristics are observed in the PFS of V0332+53:

1. Low Pulsed Fraction (PF): The PF is notably low compared to other X-ray pulsars. The geometry of the binary system relative to the observer could explain this anomaly. It is possible that our line of sight is closely aligned with the spin axis of the neutron star, while the magnetic obliquity (the angle between the spin axis and the magnetic axis) is extreme—either very small or nearly orthogonal. In the case of an orthogonal configuration, a fan beam pattern should be assumed for all observations. This could explain both the overall low PF values (likely caused by inhomogeneous reflection patterns on the neutron star from the two accretion columns as seen by the distant observer) and the large optical depth of the cyclotron line in the energy spectra. Most observed photons are detected perpendicular to the magnetic field, where the scattering/absorption cross-section for cyclotron absorption is highest. In the case of a small magnetic obliquity (less than 30°), a pencil beam pattern would be expected.

2. Peaks around the cyclotron line energy: Unlike other sources, where the PFS dips around the cyclotron line energies (e.g., Ferrigno et al. 2023), V0332+53 exhibits two peaks, one to the left and one to the right of the fundamental cyclotron line energy (∼ 28 keV). These two peaks can be modeled with two Gaussian lines of positive amplitude. We interpret them as evidence of cyclotron emission wings, as predicted by theoretical models of line formation for resonant cyclotron absorption features and their propagation along the observer's line of sight. Several theoretical models of cyclotron line absorption have shown that the absorption profile is not simply a smooth Gaussian or Lorentzian, but rather is distorted by various physical processes (Isenberg et al. 1998a; Schonherr et al. 2007; Schwarm 2017). One key prediction of these models is the presence of emission wings. These features would appear as emission on either side of a Gaussian profile, and Monte Carlo simulations have confirmed the formation of such structures around the cyclotron energy (Nishimura 1994; Isenberg et al. 1998b; Araya & Harding 1996, 1999; Schwarm et al. 2017; Kumar et al. 2022; Mushtukov et al. 2021; Sokolova-Lapa et al. 2021; Loudas et al. 2024). We interpret these features as arising from the reprocessing of cyclotron line photons—either scattered or re-emitted from higher-excited Landau levels—in the line-forming region.